Contribution from the Department of Chemistry,
McGill University, Montreal, Quebec, Canada

Vibrational Spectra and Potential Constants of the (η^6-Benzene)chromium(0) Chalcocarbonyl Complexes (η^6-C_6H_6)$Cr(CO)_2(CX)$ (X = O, S, Se)

ANN M. ENGLISH, KEITH R. PLOWMAN, and IAN S. BUTLER*

Received May 6, 1981

Infrared and laser Raman spectra have been recorded at room temperature for the ten chromium(0) chalcocarbonyl complexes $BzCr(^{12}CO)_2(^{12}CX)$, $(Bz\text{-}d_6)Cr(^{12}CO)_2(^{12}CX)$, $BzCr(^{13}CO)_3$, $BzCr(^{13}CO)_2(^{12}CS)$, $BzCr(^{13}CO)_2(^{12}CSe)$, and $BzCr(^{12}CO)_2(^{13}CS)$ (Bz = η^6-C_6H_6; X = O, S, Se), as solids and in various organic solvents. Vibrational assignments are proposed for most of the fundamental modes on the basis of general quadratic compliance and force field calculations in which the ν(CO), ν(CS), and ν(CSe) vibrations were corrected for anharmonicity. The variations observed on comparing the primary CX and CrC(X) potential constants of the $BzCr(CO)_2(CX)$ complexes with those of the related $Cr(CO)_5(CX)$ derivatives are in line with the so-called "charge buffering ability" of CS (and presumably CSe as well) originally proposed by Andrews. Also, in agreement with earlier studies on transition-metal chalcocarbonyls, the net π-acceptor/σ-donor capacity of the CX ligands increases in the order CO < CS < CSe. There is no appreciable mixing between the ν(CO) and ν(CS) or ν(CSe) modes, but there is extensive mixing between ν(CX) and the corresponding ν[CrC(X)] mode, particularly in the case of the selenocarbonyl complex. In fact, comparisons of the general quadratic and energy-factored force fields for the CX modes shows that energy factoring for the thio- and selenocarbonyl is an extremely poor approximation, and any conclusions based on such calculations will be grossly in error.

Introduction

Our continuing interest in the physicochemical properties of transition metal thio- and selenocarbonyls[1] recently led us to examine the vibrational spectra of the pentacarbonyl(chalcocarbonyl)chromium(0) complexes $Cr(CO)_5(CX)$ (X = S, Se).[2] The proposed assignments for the fundamentals were substantiated by general quadratic valence compliance and force field calculations which also enabled us to discuss the π-acceptor/σ-donor capacities of the two CX ligands more fully than previously possible. The vibrational data provided further evidence for the transferability of compliance and force constants between species of closely related geometry and showed the similarity in the bonding properties of the coordinated CS and CSe ligands. To obtain such information for the free ligands themselves is essentially impossible because CS is only stable below ~100 K,[3] while all attempts to isolate CSe, even at liquid-helium temperatures, have failed.[4] We have currently been extending our vibrational studies on metal chalcocarbonyl complexes, and, in this paper, we report the results of complete vibrational analyses of the $BzCr(CO)_2(CX)$ (Bz = η^6-C_6H_6; X = O, S, Se) complexes and their Bz-d_6 and ^{13}-C labeled derivatives.

The structures and properties of π complexes of cyclic polyenes, C_nH_n (n = 4-8), have received considerable attention over the past 25 years.[5] However, investigations of the vibrational spectra of these systems and the related "half-sandwich" complexes, (η^n-C_nH_n)ML_x, have been mainly concerned with the effects of coordination on the ring.[6] Of particular relevance to the work being presented in this paper are the normal-coordinate analyses that have been reported where L is a chalcocarbonyl ligand: $BzCr(CO)_3$[7-10] and (η^6-$CH_3CO_2C_6H_5$)$Cr(CO)_2(CX)$ (X = O, S, Se).[11]

The force constants listed in Table I indicate that the force fields reported for $BzCr(CO)_3$ vary considerably. This is in part due to the different approximations employed in the calculations. Cataliotti et al.[7] treated the benzene ring as a 78 amu point mass, while in the other analyses the molecule as a whole was considered. Both Brunvoll et al.[8] and Adams et al.[9] were primarily concerned with the differences in the force fields of free and coordinated benzene. However, their conclusions are contradictory—the former group maintains that kinematic coupling effects account for the observed wavenumber shifts on complexation, whereas the latter group showed that considerable changes in the force field of free benzene are necessary to obtain a satisfactory fit for the observed vibrational frequencies. Finally, some of the force constants obtained by Bisby and co-workers[10] seem unrealistically large when compared to those found in related molecules, e.g., the metal–carbonyl stretching force constant calculated is 3.88 mdyn Å^{-1} as opposed to 2.10 mdyn Å^{-1} in $Cr(CO)_6$ itself.

The first study in the (η^6-$CH_3CO_2C_6H_5$)$Cr(CO)_2(CX)$ series, dealing with the normal coordinate analysis of the tricarbonyl complex,[11a] appeared before we commenced work on the analogous $BzCr(CO)_2(CX)$ series. And while our work was in progress, the remaining two analyses were published.[11b,c] A complete set of internal coordinates was defined for the three molecules, and the IR and Raman spectra of the solids only were recorded. Initial force fields were estimated from previous normal-coordinate analyses of the free ligand and $Cr(CO)_6$. Although the final force fields (Table I) may seem reasonable at first glance, they are in truth only approximate owing to a number of different factors, viz., the poor wavenumber fit of many of the calculated frequencies to those observed, the lack of isotopic labeling to aid in the assignments of these complex systems, the use of solid-state data only, and the large number of unobserved fundamental modes.

(1) I. S. Butler, *Acc. Chem. Res.*, **10**, 359 (1977).
(2) A. M. English, K. R. Plowman, and I. S. Butler, *Inorg. Chem.*, **20**, 2553 (1981).
(3) K. J. Klabunde, C. M. White, and H. F. Efner, *Inorg. Chem.*, **13**, 1778 (1974) and references cited therein.
(4) R. Steudel, *Angew. Chem., Int. Ed. Engl.*, **6**, 635 (1967).
(5) (a) G. E. Coates, M. L. H. Green, and K. Wade, "Organometallic Chemistry", Vol. II, Methuen, London, 1968; (b) K. F. Purcell and J. C. Kotz, "Inorganic Chemistry", Saunders, Philadelphia, 1977 and references cited therein.
(6) (a) H. P. Fritz, *Adv. Organomet. Chem.*, **1**, 239 (1964); (b) G. Davidson, *Organomet. Chem. Rev., Sect. A*, **8**, 303 (1972); (c) K. Nakamoto, "Infrared and Raman Spectra of Inorganic and Coordination Compounds", 3rd ed., Wiley, New York, 1978; (d) E. Maslowsky, Jr., "Vibrational Spectra of Organometallic Compounds", Wiley, New York, 1977.
(7) R. Cataliotti, A. Poletti, and A. Santucci, *J. Mol. Struct.*, **5**, 215 (1970).
(8) J. Brunvoll, S. J. Cyvin, and L. Schäfer, *J. Organomet. Chem.*, **36**, 143 (1972).
(9) D. M. Adams, R. E. Christopher, and D. C. Stevens, *Inorg. Chem.*, **14**, 1562 (1975).
(10) E. M. Bisby, G. Davidson, and D. A. Duce, *J. Mol. Struct.*, **48**, 93 (1978).
(11) (a) P. Caillet, *J. Organomet. Chem.*, **102**, 481 (1975); (b) P. Caillet, *C. R. Hebd. Seances Acad. Sci., Ser. C*, **281**, 1057 (1975); (c) P. Caillet, *J. Organomet. Chem.*, **164**, 329 (1979).

0020-1669/82/1321-0338$01.25/0

Table I. Literature Values for Some Force Constants for the $M(CO)_2(CX)$ Moiety in (η^6-arene)$M(CO)_2(CX)$ (X = O, S, Se)[a]

force constant[c]	(η^6-$C_6H_6Cr(CO)_3$ (C_{3v})[b] ref 7	ref 9	ref 10	force[c,d] constant	(η^6-$CH_3CO_2C_6H_5$)$Cr(CO)_2(CX)$ X = O (C_s) ref 11a	X = S (C_1) ref 11b	X = Se (C_1) ref 11c	force[c,d] constant	(η^6-$CH_3CO_2C_6H_5$)$Cr(CO)_2(CX)$ X = O (C_s) ref 11a	X = S (C_1) ref 11b	X = Se (C_1) ref 11c
CO	13.55	14.8	14.64	CO	14.98	15.45	15.65	$MCO_\parallel$	0.84	0.84	0.84
CO,CO	0.46		0.35	CO,CO	0.25	0.25	0.25	$MCX_\perp$		0.92	0.84
MC	2.97	1.6	3.88	CX		7.30	5.90	$MCX_\parallel$		0.92	0.84
MC,MC	0.12			MC(O)	2.15	2.15	2.00	CMC(O)	0.40	0.40	0.40
MC(R)	2.37	1.3	3.74	MC,MC	−0.02	−0.02	−0.02	CMC(X)		0.60	0.60
$MCO_\perp$	1.10	0.46	0.70	MC(X)		2.30	2.70	CMC(R)	0.20	0.20	0.20
$MCO_\parallel$	1.00	0.33	0.79	MC(R)	0.75	0.75	0.65				
CMC		0.1	0.34	$MCO_\perp$	0.84	0.84	0.84				
CMC(R)		0.1	0.44								

[a] Units are mdyn $Å^{-1}$ for stretching and mdyn Å rad^{-2} for bending force constants. [b] Local symmetry of $M(CO)_2(CX)$ moiety. [c] C(R) = carbon of arene ring, except for ref 7. C(R) = "point mass"; see text. $MCO_\perp$ and $MCO_\parallel$ represent linear bending modes perpendicular and parallel to metal-ring axis, respectively. [d] Average of values given in ref 11.

The aim of the present vibrational analyses of the $BzCr(CO)_2(CX)$ series was to probe the perturbation on the remaining chalcocarbonyl groups when a benzene ring is substituted into $Cr(CO)_5(CX)$. Substitution of three carbonyl groups for an arene ring would be expected to cause a significant increase in the electron density at the chromium atom. This in turn should permit some variation in the σ-donor/π-acceptor ratios of the CX ligands. Since the MC and CX stretching force constants are sensitive to changes in these ratios, changes in the metal–ligand orbital interactions, as well as the extent of competition between the CO and CS or CSe ligands, should be reflected in the final potential fields. Any changes occurring in the ring itself on complexation will not be considered, but variation in the metal–ring interaction on descending the chalcocarbonyl series will be of importance in the present investigation.

Since the most instructive comparison will be with the potential fields previously calculated for $Cr(CO)_5(CX)$,[2] the two systems should be as self-consistent as possible. Thus, given that chromium is formally in the zero oxidation state in both series, an octahedral geometry should be used in each case. Furthermore, a model which omits the internal coordinates of the ring would greatly simplify the problem because the potential constants of complexed benzene are not desired. The model chosen for the $BzCr(CO)_2(CX)$ complexes was that of an all-cis octahedron, $L_3M(CO)_2(CX)$, where the ring is approximated by three point masses L such that L = C_2H_2 (26 amu). A total of 27 internal coordinates are necessary to describe the internal motion of this octahedron as compared to 57 for the molecule as a whole and 19 for the point ring approximation [$RCr(CO)_3$] used by Cataliotti et al.[7] Such an octahedral model for the bonding in $BzCr(CO)_2(CX)$ is supported by the published crystal structure of $BzCr(CO)_3$.[12] The OC–Cr–CO bond angle was found to be 87.76°, a value close to the octahedral bond angle of 90°. Furthermore, at 78 K, the coordinated benzene molecule has C_3 rather than C_{6v} symmetry since two different bond lengths are observed for the carbon–carbon linkages. If the metal bonding is described in terms of octahedrally directed localized orbitals, three of these would point toward the centers of the three shorter carbon–carbon bonds, placing these bonds trans to the carbonyl groups. The variation in the carbon–carbon bond lengths is indicative of partial localization of the double bonds which in turn implies partial destruction of the aromaticity of the ring.

The potential constant calculations reported here were performed by using compliance constants rather than the more familiar force constants for the reasons stated in our earlier paper.[2] However, because of the greater familiarity of chemists with force constants, these will be used in the Discussion, where the relationship between the potential constants of the $BzCr(CO)_2(CX)$ molecules and their bonding is being considered.

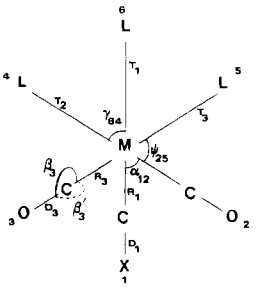

Figure 1. Internal coordinates of the $L_3M(CO)_2(CX)$ (X = O, S, Se) molecules. For X = S and Se, $R_1 = R_x$, $D_1 = D_x$, $T_1 = T_x$, $\beta_1 = \phi$, and $\beta_1' = \phi'$.

Table II. Symmetry Coordinates for $L_3M(CO)_3$ (C_{3v} Symmetry)[a]

A_1 Block

$$S_1 = (1/3^{1/2})(D_1 + D_2 + D_3)$$
$$S_2 = (1/3^{1/2})(\beta_1 + \beta_2 + \beta_3)$$
$$S_3 = (1/3^{1/2})(R_1 + R_2 + R_3)$$
$$S_4 = (1/3^{1/2})(T_1 + T_2 + T_3)$$
$$S_5 = (1/6^{1/2})(\alpha_{23} + \alpha_{12} + \alpha_{13} - \gamma_{45} - \gamma_{64} - \gamma_{65})$$
$$S_6 = (1/12^{1/2})(\psi_{25} + \psi_{34} + \psi_{14} + \psi_{26} + \psi_{15} + \psi_{36} - \alpha_{23} - \alpha_{12} - \alpha_{13} - \gamma_{45} - \gamma_{64} - \gamma_{65})$$
$$S_{Red} = (1/12^{1/2})(\psi_{25} + \psi_{34} + \psi_{14} + \psi_{26} + \psi_{15} + \psi_{36} + \alpha_{23} + \alpha_{12} + \alpha_{13} + \gamma_{45} + \gamma_{64} + \gamma_{65}) = 0$$

A_2 Block

$$S_7 = (1/3^{1/2})(\beta_1' + \beta_2' + \beta_3')$$
$$S_8 = (1/6^{1/2})(\psi_{14} - \psi_{15} + \psi_{25} - \psi_{26} + \psi_{36} + \psi_{34})$$

E Block

$$S_9 = (1/6^{1/2})(2D_1 - D_2 - D_3)$$
$$S_{10} = (1/6^{1/2})(2\beta_1 - \beta_2 - \beta_3)$$
$$S_{11} = (1/2^{1/2})(\beta_2' - \beta_3')$$
$$S_{12} = (1/6^{1/2})(2R_1 - R_2 - R_3)$$
$$S_{13} = (1/6^{1/2})(2T_1 - T_2 - T_3)$$
$$S_{14} = (1/6^{1/2})(2\alpha_{23} - \alpha_{12} - \alpha_{13} - 2\gamma_{45} + \gamma_{64} + \gamma_{65})$$
$$S_{15} = (1/24^{1/2})(2\psi_{25} + 2\psi_{34} - \psi_{14} - \psi_{26} - \psi_{15} - \psi_{36} - 2\alpha_{23} + \alpha_{12} + \alpha_{13} - 2\gamma_{45} + \gamma_{64} + \gamma_{65})$$
$$S_{16} = {}^1/_2(\psi_{14} - \psi_{26} + \psi_{15} - \psi_{36})$$
$$S_{Red} = (1/24^{1/2})(2\psi_{25} + \psi_{34} - \psi_{14} - \psi_{26} - \psi_{15} - \psi_{36} + 2\alpha_{23} - \alpha_{12} - \alpha_{13} + 2\gamma_{45} - \gamma_{64} - \gamma_{65}) = 0$$

[a] The internal coordinates and numbering of atoms are shown in Figure 1, except X = O.

Experimental Section

Materials and Instrumentation. The labeled and unlabeled complexes were prepared by the literature methods[13,14] and were sublimed

(12) B. Kees and P. Coppens, *Acta Crystallogr., Sect. B*, **B29**, 2515 (1973).

(13) A. M. English, K. R. Plowman, and I. S. Butler, *J. Labelled Compds. Radiopharm.*, **17**, 641 (1980).

Table III. Symmetry Coordinates for $L_3M(CO)_2(CX)$ (C_s Symmetry)[a-c]

A′ Block

$S_1 = (1/2^{1/2})(D_2 + D_3)$
$S_2 = D_x$
$S_3 = (1/2^{1/2})(\beta_2' - \beta_3')$
$S_4 = (1/2^{1/2})(\beta_2 + \beta_3)$
$S_5 = \phi$
$S_6 = (1/2^{1/2})(R_2 + R_3)$
$S_7 = R_x$
$S_8 = (1/2^{1/2})(T_2 + T_3)$
$S_9 = T_x$
$S_{10} = {}^1/_2(\alpha_{23} - \psi_{34} + \gamma_{45} - \psi_{25})$
$S_{11} = (1/2^{1/2})(\alpha_{23} - \gamma_{45})$
$S_{12} = {}^1/_2(\alpha_{12} + \alpha_{13} - \gamma_{64} - \gamma_{65})$
$S_{13} = {}^1/_2(\psi_{14} + \psi_{15} - \psi_{26} - \psi_{36})$
$S_{14} = (1/8^{1/2})(\alpha_{12} + \alpha_{13} + \gamma_{64} + \gamma_{65} + \psi_{14} - \psi_{15} - \psi_{26} - \psi_{36})$
$S_{Red} = (1/8^{1/2})(\alpha_{12} + \alpha_{13} + \gamma_{64} + \gamma_{65} + \psi_{14} + \psi_{15} + \psi_{26} + \psi_{36}) = 0$
$S_{Red} = {}^1/_2(\alpha_{23} + \psi_{34} + \gamma_{45} + \psi_{25}) = 0$

A″ Block

$S_{15} = (1/2^{1/2})(D_2 - D_3)$
$S_{16} = (1/2^{1/2})(\beta_2' + \beta_3')$
$S_{17} = (1/2^{1/2})(\beta_2 - \beta_3)$
$S_{18} = \phi'$
$S_{19} = (1/2^{1/2})(R_2 - R_3)$
$S_{20} = (1/2^{1/2})(T_2 - T_3)$
$S_{21} = {}^1/_2(\alpha_{12} - \alpha_{13} - \gamma_{64} + \gamma_{65})$
$S_{22} = (1/2^{1/2})(\psi_{25} - \psi_{34})$
$S_{23} = {}^1/_2(\psi_{14} - \psi_{15} - \psi_{26} + \psi_{36})$
$S_{24} = (1/8^{1/2})(\alpha_{12} - \alpha_{13} + \gamma_{64} - \gamma_{65} - \psi_{14} + \psi_{15} - \psi_{26} + \psi_{36})$
$S_{Red} = (1/8^{1/2})(\alpha_{12} - \alpha_{13} + \gamma_{64} - \gamma_{65} + \psi_{14} - \psi_{15} + \psi_{26} - \psi_{36}) = 0$

[a] See footnote to Table II. [b] For $L_3M(CO)_2(CX)$, T_1, R_1, and D_1 in Figure 1 become T_x, R_x, and D_x, respectively. [c] Under C_s symmetry, α, γ, and ψ belong to seven symmetrically nonequivalent sets (see text). The notation used for C_{3v} symmetry is retained for the sake of simplicity. The symmetrically equivalent valence angle bending modes can be readily deduced from Figure 1.

immediately prior to use. Spectrograde solvents (CS_2 and C_6H_6) were used without further purification. The IR and Raman spectra were obtained as previously reported.[2] The accuracy in the fundamental and binary ν(CO) and ν(CX) regions is ±0.5 cm^{-1} for all the complexes. In the 800–400-cm^{-1} regions of both the IR and Raman spectra, the band positions are accurate to ±1 cm^{-1} for the tricarbonyl and to only ±2–3 cm^{-1} for the dicarbonyls due to the many weak and overlapping bands for these complexes.

Internal and Symmetry Coordinates for $BzCr(CO)_2(CX)$. The internal coordinates for $BzCr(CO)_2(CX)$ in the $L_3M(CO)_2(CX)$ approximation are shown in Figure 1. The corresponding symmetry coordinates are listed in Tables II (X = O; C_{3v} symmetry) and III (X = S, Se; C_s symmetry). The symmetry coordinates are linear combinations of the 27 internal coordinates given in Figure 1. Since a ten-atom, nonlinear molecule possesses 24 vibrations, only 24 symmetry coordinates are needed; it is therefore necessary to construct three redundant symmetry coordinates. The redundancies occur in the bending coordinates as only $2n - 3$ independent angles exist about a central atom bonded to n other atoms. Thus, for $n = 6$, 9 symmetry coordinates are required though the symmetrically equivalent sets of internal coordinates consist of a total of 12 angle increments. Under C_{3v} and C_s symmetry, the redundancies have $a_1 + e$ and $a' + 2a''$ symmetries, respectively. The redundancy condition is of the form, $S_{Red} = 0$; thus, the redundant coordinates in Tables II and III are those whose sums equal 0.

Normal-Coordinate Calculations. The procedure followed in the normal-coordinate analyses of the arene complexes is the same as that used for the $Cr(CO)_5(CX)$ molecules.[2] The molecular dimensions used in the determination of the G matrix for $L_3Cr(CO)_3$ are those given in ref 12. The Cr–L distance was calculated from the C–C and Cr–C(C_6H_6) distances. Suitable bond lengths for $L_3Cr(CO)_2(CX)$ (X = S, Se) were estimated from those reported for the series (η^6-$CH_3CO_2C_6H_5$)$Cr(CO)_2(CX)$ (X = O, S, Se).[15] To allow for any differences caused by the presence of a different arene group, it was necessary to multiply the lengths obtained for the methyl benzoate chalcocarbonyls by the ratio of the lengths of the corresponding bonds in $BzCr(CO)_3$ and (η^6-$CH_3CO_2C_6H_5$)$Cr(CO)_3$. The actual values (Å) used in the calculations were as follows: $BzCr(CO)_3$, CrC = 1.845, CrL = 2.118, CO = 1.159; $BzCr(CO)_2(CS)$, CrC(O) = 1.848, CrC(S) = 1.792, CrL = 2.127, CO = 1.165, CS = 1.584; $BzCr(CO)_2(CSe)$, CrC(O) = 1.862, CrC(Se) = 1.786, CrL = 2.134, CO = 1.156, CSe 1.737. All bond angles were set equal to 90°. The atomic masses employed were the same as those given for the pentacarbonyls with the additional values for ^1H and ^2H of 1.007 825 and 2.014 10 amu, respectively. The elements of the symmetry compliance constant matrices were constructed in the manner outlined for the pentacarbonyl complexes,[2] and the diagonal elements are given in Tables 13(s) and 14(s) for the tricarbonyl (C_{3v}) and the dicarbonyl (C_s) complexes, respectively. (Note: A letter "s" following a table number means that this table is deposited as supplementary material.) The labeling of the valence compliance constants in these tables corresponds to that of the internal coordinates given in Figure 1. In the C_s complexes, the valence–angle bending coordinates belong to seven different, symmetrically nonequivalent sets: (1) α_{23}, (2) α_{13}, α_{12}, (3) γ_{45}, (4) γ_{46}, γ_{56}, (5) ψ_{14}, ψ_{15}, (6) ψ_{26}, ψ_{36}, and (7) ψ_{34}, ψ_{25}. Additional notation to distinguish each set was not introduced since these can be readily deduced from the numbering of the valence–angle coordinates.

Refinement of the $BzCr(CO)_3$ Compliant Field. The band positions input for the normal species are italicized in Table IV. The corresponding values were used for the perdeuterated and the all-^{13}O substituted complexes. For ν(CO), the harmonic frequencies listed in Table VII were input. As in the case of the pentacarbonyls, the number of general quadratic compliance constants is far in excess of the number of observed frequencies. Numerous constants must, therefore, be constrained in the refinement. Many of the $Cr(CO)_6$ interaction constants should be directly transferable to the tricarbonyl moiety since the CrCO groups are at approximately 90° to each other in both complexes. In the absence of suitable constraints from similar systems, the choice of interaction constants for the CrL_3 moiety is somewhat arbitrary. This is also true of the interactions between the $Cr(CO)_3$ and CrL_3 fragments.

As a first approximation, all diagonal and off-diagonal constants of $L_3Cr(CO)_3$ were set equal to $Cr(CO)_6$ equivalents. This initial field was then used to calculate the tricarbonyl frequencies. So that the effect of setting all interactions equal to zero could be observed, the frequencies were also calculated by using only the diagonal compliants. However, owing to the much closer frequency fit obtained with the nondiagonal field, this was judged to be a better initial estimate of the tricarbonyl potential and was allowed to refine. The ready convergence of this field to within ±1 cm^{-1} of the observed band positions on refinement of the primary constants only [Table 17(s)] was rather unexpected but indicates nonetheless that the initial interaction constants are reasonable estimates of the tricarbonyl values. Furthermore, the changes in the primary constants from their initial [or $Cr(CO)_6$] values were quite reasonable from a chemical standpoint. Subsequent attempts to refine the (MC, CO) interaction together with the MC primary gave a converging field with negligible changes in the constants. A similar result was obtained when refinement of the (ML, MC) interaction with either the ML or MC primary was undertaken.

Thus, on the basis of the good wavenumber fit and the "reasonable" values obtained for the refined compliants, this solution is considered to be a good estimate of the tricarbonyl compliant field. Moreover, it should allow a fairly valid comparison of the tricarbonyl and hexacarbonyl compliance (or force) constants. The initial and refined symmetry compliants are given in Table 15(s). The valence compliance and force constants are listed in Table 18(s) and Table VIII, respectively. Only those valence constants which were elements of the "on-diagonal" symmetry constants are listed since all "off-diagonal" symmetry constants were constrained to the values of their $Cr(CO)_6$ equivalents. The estimated errors are also given in Table 18(s) for the refined constants.

(14) (a) I. S. Butler, A. M. English, and K. R. Plowman, *Inorg. Synth.*, in press; (b) A. M. English, Ph.D. Thesis, McGill University, Montreal, Quebec, Canada, 1980.

(15) (a) J. Y. Saillard and D. Grandjean, *Acta Crystallogr., Sect. B*, **B32**, 2285 (1976); (b) J. Y. Saillard, G. Le Borgne, and D. Grandjean, *J. Organomet. Chem.*, **94**, 409 (1973). (c) J. Y. Saillard and D. Grandjean, *Acta Crystallogr., Sect. B*, **B34**, 3772 (1978).

Table IV. Observed Wavenumbers in the ν(CO) Fundamental and Binary Combination Regions and in the Low-Energy Region of (η^6-C_6H_6)$Cr(CO)_3$[c]

$BzCr(CO)_3$[d]			$(Bz\text{-}d_6)Cr(CO)_3$			$BzCr(^{13}CO)_3$			
IR	Raman		IR	Raman		IR	Raman		
CS_2 soln	solid	C_6H_6 soln	CS_2 soln	solid	C_6H_6 soln	CS_2 soln	solid	C_6H_6 soln	assignts[a]
3944 w			3944 w			3856 w			$2\nu_1$
3866 w			3865 w			3778 w			$\nu_1 + \nu_2$
3798 w			3797 w			3711 w			$2\nu_2$
1976 s	1942 m	1970 p	1975 s	1942 ms	1974 p	1931 s	1897 s	1930 p	ν(CO) a_1 ν_1
1904 s	1886 ms	1893 dp	1904 s	1886 s	1897 p	1860 s	1843 s	1854 dp	ν(CO) e ν_9
	1863 s			1863 ms			1823 s		ν(CO)
647 w						647 w			
653 ms	660 ms	650 p	671 ms	674 ms	678 p	640 ms	643 ms	641 p	$\delta(MCO)_\perp$ a_1 ν_2
624 ms	636 w		622 ms	632 m		608 m			$\delta(MCO)_\parallel$ e ν_{10}
615 sh	612 w		572 m			617 w, sh	614 w		α(CCC) e
				588 s	586 p				γ(CD) a_1
532 m	537 m	536 dp	529 m	534 m	532 dp ?	517 m	522 m	518 dp ?	$\delta(MCO)_\perp$ e ν_{11}
	484 s	*478* p		484 s	477 p		476 s	470 p	ν(MC) a_1 ν_3
471 mw			472 mw			465 mw			ν(MC) e ν_{12}
	423 w			384 m			425 w		τ(CCCC)
	328 ms	*335* dp		310 ms	313 dp		329 s	334 dp	ν(ML) e ν_{13}
	295 vs	*302* dp		284 vs	291 p		294 s	301 p	ν(ML) a_1 ν_4
	270 w			266 m					
	131 vs			130 vs			130 vs		
	108 vs			108 vs			108 vs		[b] a: ν_5, ν_6; e: ν_{14}, ν_{15}, ν_{16}
	61 ms			60 s			62 s		
	46 ms			45 s			45 s		

[a] The spectra were analyzed on the basis of the approximate model (see text); therefore, the observed bands (other than those which arise from ring vibrations) are assigned to the symmetry coordinates given in Table II. [b] These peaks are due to vibrations involving strong mixtures of several different coordinates as can be seen from the PED given in Table X. [c] The italicized frequencies of the normal species and those in the corresponding columns of the labeled species were input to the normal-coordinate analysis. [d] Bz = (η^6-C_6H_6). Bz-d_6 = (η^6-C_6D_6).

Refinement of the $BzCr(CO)_2(CX)$ (X = S, Se) Compliant Fields. The low symmetry of these complexes leads to a large increase in the number of potential constants. The A′ block contains 14 primary and 91 interaction constants and the A″ block 10 primary and 45 interaction constants. Thus, only refinement of the diagonal elements was attempted for these systems. The preliminary fields are estimated from the tricarbonyl data, except for the CrCX grouping. The initial values for the ν(CX) and ν[CrC(X)] constants were taken from the pentacarbonyl complexes. The diagonal elements of the symmetry compliant matrix for $L_3Cr(CO)_2(CX)$ are given in Table 14(s). The input wavenumbers for the normal species are italicized in Tables V and VI. Again, the corresponding values were input for the deuterated and ^{13}CO-labeled species, together with the harmonic frequencies for the ν(CO) and ν(CX) modes listed in Table VII. Refinement was attempted for several alternative frequency assignments of the linear bending and metal–ligand stretching vibrations. For each complex, two or three of these alternative assignments resulted in converging fields. The set of potential constants finally selected in each case was that which yielded both a good fit of the observed frequencies and reasonable values for the valence constants when compared with those of $BzCr(CO)_3$ and $Cr(CO)_5(CX)$.

The initial and final symmetry compliants are given in Table 16(s), and the errors in the calculated wavenumbers are listed in Table 17(s). The poorer overall fit obtained for the dicarbonyls compared to the tricarbonyl is partly due to the greater difficulty in estimating the maxima of the weak and overlapping peaks in the spectra of the former. Furthermore, the criterion of convergence in the C_s calculations was that no calculated compliant correction exceeded by more than 5% the value of the compliant, whereas in the tricarbonyl the corrections were ≤1% of the compliants. The calculated wavenumbers are given for modes which were not observed or which were given zero weight due to large uncertainties in their peak positions. All valence-angle bending modes were set to zero in the C_s complexes and the corresponding compliants were constrained to their tricarbonyl values. Also, since no frequency was assigned to the unique chromium–ring stretch (ML′), a suitable constrant was estimated for the ML′ compliant from the tricarbonyl equivalent.

Results and Discussion

Observed Spectra. $BzCr(CO)_3$. The IR and Raman spectra of $BzCr(CO)_3$ have been studied by various groups,[7-10] and for the most part the assignments are satisfactory. For the calculations performed in this work, IR (CS_2 solution) and Raman (solid and C_6H_6 solution) data for the normal, perdeuterated, and all-^{13}CO-substituted species were obtained. The regions examined were limited to the CO fundamental and binary regions and the low-energy region from ~800 to 40 cm^{-1}. These regions contain all the frequencies necessary for analyses using the $L_3M(CO)_2(CX)$ model discussed earlier.

The IR spectrum of the CS_2 solution and the Raman spectrum of the solid below 1500 cm^{-1} are shown in Figure 2, while the actual band positions and proposed assignments for all the various species are collected together in Table IV. The assignment and numbering of the vibrations are based on the $L_3M(CO)_3$ model, so the ring modes which appear in the low-energy region are not numbered. The predicted vibrational modes and their symmetries are as follows: ν(CO), a_1 + e; δ(MCO), a_1 + a_2 + 2 e; ν(MC), a_1 + e; ν(ML), a_1 + e; δ(CMC) + δ(LMC) + δ(LML), 2 a_1 + a_2 + 3 e). The assignments for the carbonyl fragment are in complete agreement with those of Adams et al.[9] The extra data from the all-^{13}CO-substituted molecule confirm many of the previous assignments since the δ(MCO) and ν(MC) modes assigned by Adams et al. all exhibit the expected isotopic behavior. However, one anomaly stands out; the wavenumber increase observed (here and previously[9,10]) on deuteration for the band assigned to the a_1 in-phase δ(MCO) mode suggests that either the normal-mode description in the deuterated and undeuterated species is somewhat different or that configuration interaction causes the frequency shift. Since the previous calculations on the complete molecule[9,10] gave a poor fit for this band in the deuterated molecule, the possibility of configuration interaction in the deuterated species was investigated. In benzene and deuteriobenzene, the a_2 γ(CH) and γ(CD) modes are observed at 673 and 496 cm^{-1}, respectively.[9] On coordination, these modes show large wavenumber increases and are assigned to polarized bands at 791 and 588 cm^{-1} in the Raman spectra of the benzene solutions. However, the wavenumber shift on coordination is less in the deuterated complex since a comparable shift would give a band at 614

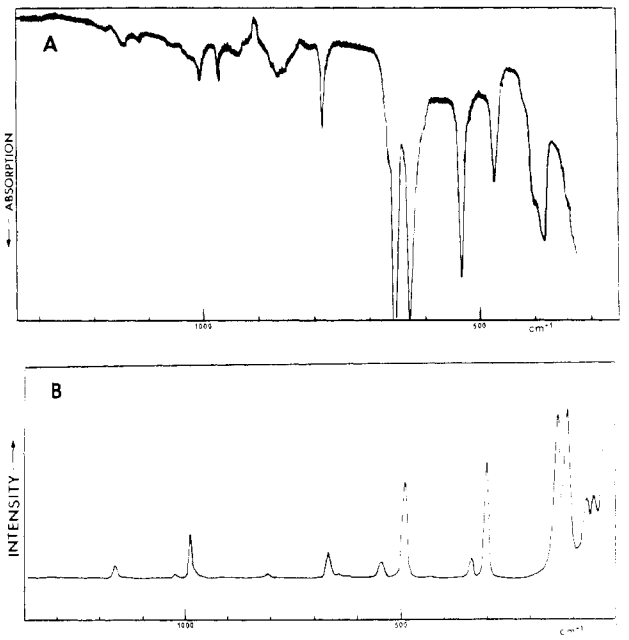

Figure 2. Vibrational spectra of $BzCr(CO)_3$ in the region below 1500 cm^{-1}. (A) IR spectrum (CS_2 solution, 0.2-mm KBr cells); (B) Raman spectrum of the solid. Conditions: slit widths, 5 cm^{-1}; sensitivity, 2×10^4 counts s^{-1}; time constant, 1 s; scan speed, 50 cm^{-1} min^{-1}; excitation, Kr^+ laser (568.1 nm, 25 mW).

cm^{-1}. Furthermore, the δ(MCO) mode loses considerable intensity on deuteration whereas γ(CD) is almost twice as intense as γ(CH). Such observations are indicative of configuration interaction which causes modes of the same symmetry and similar energies to diverge and share intensity.[16] A similar phenomenon was observed for $CpMn(CO)_3$ and its perdeuterated derivative.[17]

In the assignment of the angle bending region (150–40 cm^{-1}), the calculated values were relied upon heavily. However, the experimental and calculated wavenumbers are in good agreement. Finally, anharmonicity constants and harmonic frequencies for the two ν(CO) modes were calculated from the observed overtone and combination bands reported previously.[18]

$BzCr(CO)_2(CX)$ (X = S, Se). Again, the normal, perdeuterated and all-^{13}CO isotropic species were examined. For the thiocarbonyl complex, the additional ^{13}CS-labeled molecule was available. The IR spectra of the CS_2 solutions and the Raman spectra of the solids were recorded for all species. Raman spectra of C_6H_6 solutions of only the thiocarbonyl complexes were obtained as the selenocarbonyl solutions decomposed rapidly in the laser beam.

The spectra were analyzed in the ν(CO) and ν(CX) fundamental and binary regions and from 800 to 40 cm^{-1}. Survey scans of the IR and Raman spectra of the normal species below 1500 cm^{-1} are shown in Figures 3 and 4, while the band positions and the proposed assignments are listed in Tables V and VI. As before, analysis of the spectra was based on the octahedral model discussed above. For $L_3M(CO)_2(CX)$ under C_s symmetry, the following modes are expected: ν(CO), a′ + a″; ν(CX), a′; δ(MCO), 2 a′ + 2 a″; δ(MCX), a′ + a″; ν[MC(O)], a′ + a″; ν[MC(X)], a′; ν(ML), a′ + a′; ν(ML′), a′; and nine valence–angle bending modes, 5 a′ + 4 a″). (*Note*: ML and ML′ are trans to the MCO and MCX groups, respectively.)

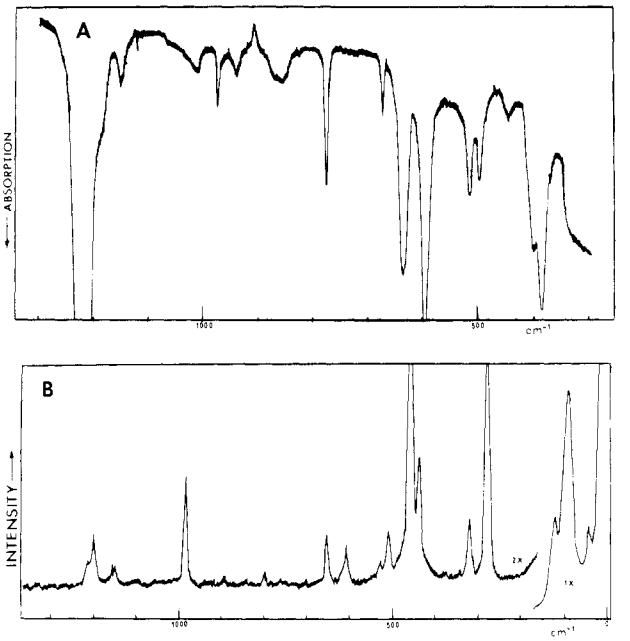

Figure 3. Vibrational spectra of $BzCr(CO)_2(CS)$ in the region below 1500 cm^{-1}: (A) IR spectrum in CS_2 solution; (B) Raman spectrum of the solid. The conditions were the same as those given in Figure 2, except that the Raman sensitivity was 2.5×10^2 counts s^{-1}.

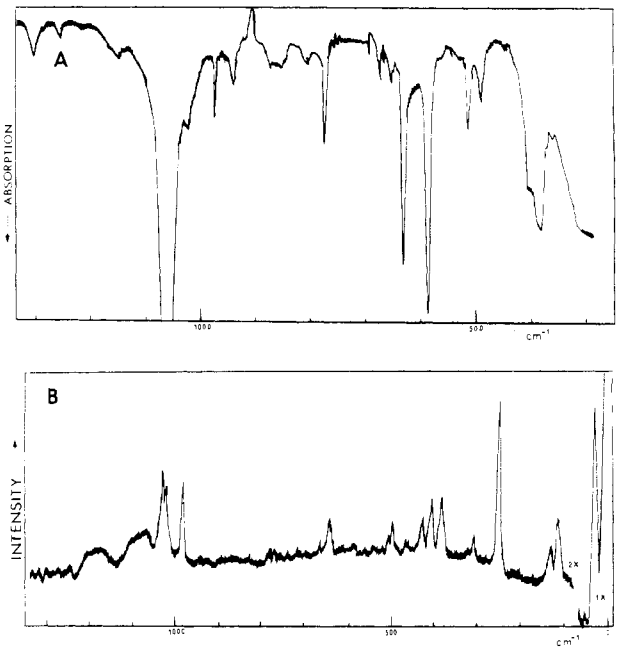

Figure 4. Vibrational spectra of $BzCr(CO)_2(CSe)$ in the region below 1500 cm^{-1}: (A) IR spectrum in CS_2 solution; (B) Raman spectrum of the solid. The conditions were the same as those given in Figure 3, except that the laser power used to obtain the Raman spectrum was 15 mW.

The ν(CO) and ν(CX) fundamental and binary regions were readily assigned on the basis of C_s symmetry. The two ν(CO) fundamentals were attributed to the a′ and a″ modes in order of decreasing energy. As observed for the pentacarbonyl complexes,[2] the ν(CS) and ν(CSe) fundamentals were found to be strongly IR active and only weakly Raman active.

The main difficulties arose in the assignment of the low-energy regions. Even with extra data available from the isotopic species, many alternative assignments of the ν(MC), δ(MCO), and δ(MCX) modes were possible. Bands exhibiting large shifts on ^{13}O substitution occurred between 650 and 480 cm^{-1}, while those with the smaller shifts typical of ν(MC)

(16) E. B. Wilson, J. C. Decius, and P. C. Cross, "Molecular Vibrations", McGraw-Hill, New York, 1955.
(17) D. J. Parker, *J. Chem. Soc., Dalton Trans.*, 155 (1974).
(18) A. M. English, J. Sedman, K. R. Plowman, and I. S. Butler, to be published.

Table V. Observed Wavenumbers in the ν(CO) and ν(CS) Fundamental and Binary Combination Regions and in the Low-Energy Region of (η^6-C_6H_6)$Cr(CO)_2$(CS)[c]

$BzCr(CO)_2(CS)$[d]			$(Bz\text{-}d_6)Cr(CO)_2(CS)$			$BzCr(^{13}CO)_2(CS)$			$BzCr(CO)_2(^{13}CS)$			
IR	Raman		IR	Raman		IR	Raman		IR	Raman		
CS_2 soln	solid	C_6H_6 soln	CS_2 soln	solid	C_6H_6 soln	CS_2 soln	solid	C_6H_6 soln	CS_2 soln	solid	C_6H_6 soln	assigns[a]
3925 w			3925 w						3926 w			$2\nu_1$
3867 w			3866 w						3866 w			$\nu_1 + \nu_{15}$
3835 w			3834 w						3835 w			$2\nu_{15}$
2424 w			2423 w						2362 w			$2\nu_2$
1969 s	1977 m	1973 p	1969 s	1978 m	1969 p	1924 s	1910 w		1969 s			ν(CO) a′ ν_1
1923 s	1953 m	1924 dp	1923 s	1963 w	1921 dp	1880 s	1849 w		1923 s			ν(CO) a″ ν_{15}
	1892 m			1931 w								
1220 s	1207 w	1223 p	1220 s	1203 w	1221 p	1221 s	1208 w		1182 n	1175 w		ν(CS) a′ ν_2
	1194 w			1188 w			1197 w			1132 w		
637 m	646 mw	645 p	648 m	656 mw	656 p	638 m	638 m		636 m	646 mw	643 p	$\delta(MCO)_\perp$ a′ ν_3
600 m	603 mw		602 m	604 mw		589 m	590 m		599 m	602 mw		$\delta(MCO)_\perp$ a″ ν_{16}
597 m, sh			598 m, sh			594 m, sh			589 m, sh			$\delta(MCO)_\parallel$ a′ ν_4
				581 s	580 p							γ(CD)
517 mw	521 w		515 mw	521 w		510 mw			516 mw			$\delta(MCS)_\parallel$ a′ ν_5
517 mw						502 mw						$\delta(MCO)_\parallel$ a″ ν_{17}
499 mw	502 mw	502 ?	497 mw	502 mw	502 ?	492 mw	497 mw		495 mw	502 mw		$\delta(MCS)_\perp$ a″ ν_{18}
452 w, sh	452 vs	*449 p*	450 w, sh	450 vs	449 p	446 w, sh	448 vs	446 p	452 w, sh	450 s	449 p	ν[MC(O)] a′ ν_6
443 w			443 w			439 w			442 w			ν[MC(O)] a″ ν_{19}
	433 m		431 m			431 m			428 m			ν[MC(S)] a′ ν_7
				372 m	380 dp							τ(CCCC)
	314 mw	321 dp		298 mw	302 dp		315 mw	322 dp		316 mw	319 dp	ν(ML) a″ ν_{20}
	272 vs	273 p		265 vs	280 p		272 vs	275 p		272 vs	275 p	ν(ML) a′ ν_8
	121 s, sh			121 s, sh			121 s, sh			121 s, sh		a′, ν_{10}, ν_{11}, ν_{12}
	112 s, sh			112 s, sh			112 s, sh			114 s, sh		[b] ν_{13}, ν_{14}
	84 s			84 s			84 s			85 s		a″, ν_{21}, ν_{22}, ν_{23}
	35 s			35 s			34 s			34 s		ν_{24}

[a] See footnotes *a–d* in Table IV.

modes fell between 460 and 230 cm^{-1}. Also, the latter modes were relatively weak in the IR and strong in the Raman, whereas the former exhibited the reverse pattern. Such intensity[19] and isotopic behavior[20] suggest that the higher energy bands should be assigned to linear bending modes and the lower energy ones to metal–ligand stretches. The assignments given in Tables V and VI are those considered to yield the most acceptable potential constants. However, since the potential energy distributions (Table XI) show that many of the modes are strongly mixed, even these assignments represent an oversimplification. For example, the calculated mixing of ν(MCO) and δ(MCX) from the PED's reveals that these modes are almost completely mixed; this explains the unexpected shift of ν(MCX) on ^{13}CO substitution and the shift of ν(MCO) on ^{13}CS substitution which complicate the low-energy assignments.

Strong and medium-intense bands observed in the Raman spectrum of the unlabeled, solid thiocarbonyl at 452 and 433 cm^{-1} are assigned to the ν[MC(O)] and ν[MC(S)] a′ modes, respectively. A broad, asymmetric, polarized band, corresponding to these two solid-state bands, appears at 449 cm^{-1} in the Raman spectrum of the C_6H_6 solution. A weak IR band at 443 cm^{-1} is assigned to the ν[MC(O)] a″ mode. The ν(ML) modes are easily identified because of their large shifts on deuteration.

The lack of Raman spectra for the solutions of the selenocarbonyl complexes makes the detailed assignment of the metal–ligand stretching regions in these complexes more tentative. The two strong bands observed below 300 cm^{-1} are attributed to the a″ and a′ ν(ML) modes in order of decreasing energy. This leaves two medium-intense bands (at 407 and 383 cm^{-1} in the normal species and at 407 and 381 cm^{-1} in the ^{13}CO species) which are ascribed to the low-energy ring torsion mode, τ(CCCC), and the a′ ν[MC(Se)] mode, respectively, since on deuteration the 407-cm^{-1} peak shifts to 377 cm^{-1} while the other remains at 381 cm^{-1}.

The a′ and a″ ν[MC(O)] modes are both assigned to a broad, medium-intense band at 429 cm^{-1} in the Raman spectrum of solid $BzCr(CO)_2(CSe)$ and a corresponding peak at 426 cm^{-1} for the ^{13}CO-labeled species supports this assignment. In the deuterated species, however, a band is observed at 420 cm^{-1} which is smaller in shape and intensity to that at 429 cm^{-1} in the normal species. Such a large shift on deuteration is not expected unless lattice or resonance interactions are perturbing the internal modes of this species.

A very weak band appears at 450 cm^{-1} in the IR spectra of the normal species which was initially assigned to the a″ ν[MC(O)] mode. However, this resulted in a diverging field with unacceptable values for some of the potential constants while, in fact, the band can be easily accounted for by a combination of two fundamental modes (Table VI).

Valence Potential Constants. The valence force and compliance constants for $BzCr(CO)_2(CX)$ (X = O, S, Se) are listed in Tables VIII and 18(s), together with the equivalent values for $Cr(CO)_6$ and $Cr(CO)_5(CX)$. The force constants were obtained from the inverse compliance constant matrix, $\mathbf{F} = C^{-1}$. Only those compliants (and the corresponding force constants) which were allowed to refine are given here. The remaining compliants have the same value as their $Cr(CO)_6$ counterparts.

A comparison of the hexacarbonyl and tricarbonyl data in Table VIII reveals that substitution of three carbonyl groups in $Cr(CO)_6$ leads to a considerable decrease in the ν(CO) force constant and an increase in the ν(MC) constant. Such changes

(19) (a) G. Davidson, *Inorg. Chim. Acta*, **3**, 596 (1969); (b) D. M. Adams and A. Squire, *J. Chem. Soc. A*, 814 (1970).
(20) L. H. Jones, R. S. McDowell, and M. Goldblatt, *Inorg. Chem.*, **8**, 2349 (1969).

Table VI. Observed Wavenumbers in the ν(CO) and ν(CSe) Fundamental and Binary Combination Regions and in the Low-Energy Region of $(\eta^6\text{-}C_6H_6)Cr(CO)_2(CSe)$[c]

$BzCr(CO)_2(CSe)$[d]		$(Bz\text{-}d_6)Cr(CO)_2(CSe)$		$BzCr(^{13}CO)_2(CSe)$		
IR CS_2 soln	Raman solid	IR CS_2 soln	Raman solid	IR CS_2 soln	Raman solid	assignts[a]
3939 w						$2\nu_1$
3880 w						$\nu_1 + \nu_{15}$
3851 w						$2\nu_{15}$
1975 s	1937 w	1975 s	1937 w	1930 s	1987 w	ν(CO) a′ ν_1
1932 s	1912 w	1931 s	1911 w	1888 s	1872 w	ν(CO) a″ ν_{15}
1061 s	1028 w	1062 s	1030 w	1061 s	1027 w	ν(CSe) a′ ν_2
	1018 w				1018 w	
634 m	640 mw	643 m	647 m	624 m	630 m	$\delta(MCO)_\perp$ a′ ν_3
613 w		570 m		613 w, sh		α(CCC)
586 m		589 m		573 m		$\delta(MCO)_\parallel$ a′ ν_4
586 m				582 m		$\delta(MCO)_\perp$ a″ ν_{16}
			577 w			γ(CD)
513 mw		511 m		497 m		$\delta(MCO)_\parallel$ a″ ν_{17}
513 mw				504 m		$\delta(MCSe)_\parallel$ a′ ν_5
491 mw	496 m	489 m	495 m	483 m	486 m	$\delta(MCSe)_\perp$ a″ ν_{18}
450 vvw		450 vvw		441 vvw		ν_7 + CMC
	429 m, br		420 m, br		426 m, br	ν[MC(O)] a′, a″ ν_6, ν_{19}
	407 m		377 m		407 m	τ(CCCC)
	383 m		381 m		381 m	ν[MC(Se)] a′ ν_7
			300 w		319 w	ν_8 + CMC
	306 mw		287 mw		304 mw	ν(ML) a″ ν_{20}
	249 vs		238 vs		248 vs	ν(ML) a′ ν_8
	131 s, sh				130 s, sh	b a′: ν_{10}, ν_{11}, ν_{12}, ν_{13}, ν_{14}
	127 s, sh				125 s, sh	
	113 s		113 s		112 s	b a″: ν_{21}, ν_{22}, ν_{23}, ν_{24}
	65 vs		65 vs		64 vs	

[a] See footnotes *a–d* in Table IV.

Table VII. Harmonic Frequencies (cm^{-1}) and Anharmonicity Constants (mdyn $Å^{-1}$) for the ν(CO) and ν(CX) Modes of the $(\eta^6\text{-}C_6H_6)Cr(CO)_2(CX)$ (X = O, S, Se) Molecules in CS_2 Solution[a]

ω_i and $X_{i,j}$	$BzCr(CO)_3$		ω_i and $X_{i,j}$	$BzCr(CO)_2(CS)$			$BzCr(CO)_2(CSe)$	
	^{12}CO	^{13}CO		^{12}CO	^{13}CO	^{13}CS	^{12}CO	^{13}CO
ω_1 (a_1)	1998	1952	ω_1 a′	1995	1948	1995	2001	1955
ω_9 (e)	1927	1882	ω_{15} a″	1948	1903	1948	1957	1912
			ω_2 a′	1236	1237	1196	1073	1073
$X_{1,1}$	−3.8	−3.5	$X_{1,1}$	−6.8	−6.2	−6.3	−6.1	−5.8
$X_{9,9}$	−5.2	−5.0	$X_{15,15}$	−5.9	−5.5	−5.7	−6.0	−5.7
$X_{1,9}$	−14.2	−13.5	$X_{1,15}$	−26.2	−24.9	−26.3	−26.9	−25.7
			$X_{2,2}$	−8.0	−8.0	−7.4	−6.0	−6.0

[a] The $X_{i,j}$ for the ^{13}CO-substituted thio- and selenocarbonyl complexes were determined from those of the normal species (see ref 14b, page 71).

indicate a substantial increase in the amount of π back-bonding to the π^* orbitals of the ligands; this in turn implies that there is less competition for the metal dπ electrons in the arene compound compared to that in the hexacarbonyl. The large increase in the δ(MCO) constant can also be attributed to an increase in π back-bonding since a stronger MC bond should increase the rigidity of the MCO group.

In the thio- and selenocarbonyls, F_{CO} and $F_{MC(O)}$ become progressively larger and smaller, respectively, than in the tricarbonyl. Also, the δ(MCO) force constants decrease from the tri- to the dicarbonyls; the average of F_β and $F_{\beta'}$ going down the series are 0.720, 0.651, and 0.618 mdyn Å rad^{-2}. On the other hand, the constants for δ(MCX), as well as those for ν(CX) and ν[MC(X)], exhibit the reverse trend as X varies from O to S to Se. By comparing these constants with corresponding values for $Cr(CO)_5(CX)$[2], it is apparent that the arene complexes possess much stronger MC(X) bonds and much weaker CX bonds. Thus, the π acceptance of CX is significantly greater in $BzCr(CO)_2(CX)$ than in $Cr(CO)_5$-(CX). Furthermore, the presence of CX in the benzene compounds causes a reduction in the π back-bonding to the remaining carbonyls, as indicated by the increase in the ν(CO) force constants. These findings are compatible with the "charge buffering effect" of CS postulated by Andrews,[21] who

Table VIII. Valence Force Constants for the $(\eta^6\text{-}C_6H_6)Cr(CO)_2(CX)$ (X = O, S, Se) Molecules and the $Cr(CO)_6$ Equivalents[a]

F[b,c]	$BzCr(CO)_3$	$BzCr(CO)_2(CS)$	$BzCr(CO)_2(CSe)$	$Cr(CO)_6$[d]
F_D	15.41	15.77	15.89	17.04
F_{D_X}		6.528	4.757	7.677, 5.768
F_R	2.40	2.14	2.04	2.10
F_{R_X}		3.26	3.44	2.45, 2.66
F_T	1.19	1.04	0.897	
F_{T_X}		1.12	1.01	
F_{DD}	0.3021	0.314	0.305	0.169
F_{RR}	0.285	0.005	−0.045	−0.020
F_{TT}	−0.096	−0.138	−0.159	
F_β	0.627	0.597	0.537	0.460
$F_{\beta'}$	0.813	0.705	0.699	0.460
F_ϕ		0.706	0.816	0.48, 0.60
$F_{\phi'}$		0.939	1.08	
$F_{\beta\beta}$	0.00	0.03	0.044	0.00
$F_{\beta'\beta'}$	0.00	0.04	0.053	0.00
$F_{\alpha\gamma}$	0.31	0.28	0.28	0.55
$F_{\alpha\gamma\psi}$	0.31	0.39	0.39	0.59
$F_{\psi'}$	0.47	0.51	0.51	0.55
$F_{\alpha\gamma}$*		0.27	0.27	
$F_{\alpha\gamma\psi}$*		0.37	0.36	
$F_{\psi'}$*		0.50	0.50	
$F_{\alpha\gamma,\alpha\gamma}$	0.04	0.04	0.04	0.08
$F_{\alpha\gamma\psi,\alpha\gamma\psi}$	0.31	−0.09	−0.09	0.08
$F_{\psi'\psi'}$	0.10	0.10	0.10	0.16

[a] Units are mdyn $Å^{-1}$ for stretching and mdyn Å rad^{-2} for bending force constants. Values for F from C^{-1}. [b] For an explanation of the subscripts and asterisks employed with the valence angle bneding force constants (i.e., $F_{\alpha\gamma} - F_{\psi'\psi'}$, see footnote *a*, Table 13 (s) and footnote *c*, Table 14 (s), respectively. [c] The C_i corresponding to the F_i given here appear in Table 18 (s). This table also indicates those C_i held constant in the refinements. [d] F_i values from ref 20 except for $i = D_X$, R_X, ϕ (ref 2) and $i = \alpha\gamma - \psi'\psi'$ (ref 31).

concluded after comparing the ν(CO) and ν(CS) frequencies of various complexes that the π-acceptor/σ-donor ratio for coordinated CS can be either smaller or larger than that for coordinated CO, implying a greater adaptability of CS to its environment. The soft CSe group should also be able to withstand greater variations in charge density than the harder CO group as the results here suggest. In contrast, the results obtained for (η^6-$CH_3CO_2C_6H_5$)$Cr(CO)_2(CX)$[11] (Table I), when compared to those for $Cr(CO)_5(CX)$, indicate that the π back-bonding to CS and CSe is comparable in the two series. This is an unlikely result since the π back-donation to the methyl benzoate ring is not expected to be equal to that donated to three carbonyl groups.

The values obtained for the metal–ring constants (F_T) for the three complexes show that the metal–ring interaction becomes progressively weaker on substitution of CO by CS and then CSe. This is reflected in the relative ease of removal of the ring in the thio- and selenocarbonyls compared to the tricarbonyl.[14] However, comparing this constant with those obtained previously (Table I) is not very meaningful because the metal–ring bonding was approximated by a metal–"point mass" interaction in one model[7] and by six metal–carbon bonds in the other.[8-11] Nevertheless, the relative magnitudes of the ν(ML) and ν[MC(O)] force constants agree with the theoretical picture of the bonding in $BzCr(CO)_3$. Molecular orbital analysis of $BzCr(CO)_3$[22] indicates that the molecule is best described as a $Cr(CO)_3$ fragment interacting with a benzene ring, i.e., the complex is viewed as one in which the metal–carbonyl interaction dominates the metal–ring interaction.

Comparison of the Potential Constants, Interaction Coordinates, and Electronic Structures of the $BzCr(CO)_2(CX)$ and $Cr(CO)_5(CX)$ (X = O, S, Se) Molecules. The chief purpose of the vibrational analyses of the $BzCr(CO)_2(CX)$ series was to probe the effects of the benzene ring on the chalcocarbonyl fragments. Hence, a correlation of the differences in the electronic structures of $Cr(CO)_5(CX)$ and $BzCr(CO)_2(CX)$ with differences in their potential constants is appropriate.

Several approximate MO calculations for $BzCr(CO)_3$ have been published,[23-27] and they lead to different interpretations of the nature of the bonding in this complex. Thus, for a valid comparison of the electronic structures of $BzCr(CO)_3$ and $Cr(CO)_6$, the calculations have to be carried out with a method which is consistent in its application to both molecules. Fortunately, Brown and Rawlinson,[23,28] as well as Carroll and McGlynn,[24] have reported comparative studies on both complexes using self-consistent semiempirical methods. Although the results obtained by the two groups differ in some respects, the same general features emerge. Both calculations reveal a net positive charge on the ring. Also, in $BzCr(CO)_3$, the metal has a smaller positive charge and the CO groups a greater negative charge than in $Cr(CO)_6$. Thus, net donation of charge from the ring to the tricarbonyl fragment is suggested. This is further supported by the X-ray photoelectron studies; the 1s binding energy of the carbonyl carbon is lower in $BzCr(CO)_3$ compared to $Cr(O)_6$, while the 1s binding energies of the benzene carbons increase on complexation.[29] Since a decrease in core binding energy corresponds to an increase in the atomic electron density, the inference again is that a flow of charge from the ring to the CO groups takes place.

In addition to charge donation from the ring, the replacement of three CO groups in $Cr(CO)_6$ should substantially reduce the competition for dπ electron density among the remaining CO's. This expectation is borne out by the relative populations of the carbonyl π^* orbitals calculated by Brown and Rawlinson, who obtained values of 0.107 and 0.142 for $Cr(CO)_6$ and $BzCr(CO)_3$, respectively. By comparison, the populations of the 5σ donor orbitals are essentially unchanged, the values obtained being 1.99 for $Cr(CO)_6$ and 1.98 for $BzCr(CO)_3$. Consequently, the large difference in the general quadratic CO force constants of the two complexes [15.41 and 17.04 mdyn $Å^{-1}$ for $BzCr(CO)_3$ and $Cr(CO)_6$, respectively] can be attributed to the relative occupancies of the CO π^* orbitals in these molecules.

MC and CO overlap populations have also been reported for both $Cr(CO)_6$ and $BzCr(CO)_3$. Brown and Rawlinson[23,28] calculated MC overlap populations of 0.4978 and 0.7232 for $BzCr(CO)_3$ and $Cr(CO)_6$, respectively, implying a weaker MC stretching force constant for the benzene complex. The vibrational analyses, however, yielded a value of 2.10 mdyn $Å^{-1}$ for the MC force constant in $Cr(CO)_6$ vs. 2.40 mdyn $Å^{-1}$ for $BzCr(CO)_3$. Furthermore, although the small difference in the CO overlap populations [1.678 for $Cr(CO)_6$ and 1.630 for $BzCr(CO)_3$] obtained by these workers is in the right direction, it does not reflect the substantial difference in the CO stretching force constants of the two complexes. The overlap populations determined by Carroll and McGlynn[24] correlate much better with the force constants. For $Cr(CO)_6$, the MC and CO overlap populations are 0.415 and 1.317, respectively, while the corresponding values for $BzCr(CO)_3$ are 0.537 and 1.216.

Substitution of one CO group in $BzCr(CO)_3$ by either CS or CSe has results similar to those observed for the $Cr(CO)_6 \rightarrow Cr(CO)_5(CX)$ system. However, the effects of CX substitution are more pronounced here becauser larger differences are found for the remaining CO potential constants (Table VIII). For example, the CO stretching force constant varies from 15.41 mdyn $Å^{-1}$ in the tricarbonyl to 15.89 mdyn $Å^{-1}$ in the selenocarbonyl; the thiocarbonyl has an intermediate value of 15.77 mdyn $Å^{-1}$. The corresponding range in the MC(O) stretching constants is 2.40–2.04 mdyn $Å^{-1}$.

The effects of benzene substitution on the MCS and MCSe groupings are even greater than its effect on the MCO grouping. In the thiocarbonyl complexes, for example, F_{R_x} increases from 2.45 mdyn $Å^{-1}$ in $Cr(CO)_5(CS)$ to 3.26 mdyn $Å^{-1}$ in $BzCr(CO)_2(CS)$, while F_{D_x} decreases from 7.677 to 6.528 mdyn $Å^{-1}$. The changes obtained for the MCSe force constants are even greater. These results clearly indicate a substantial enhancement of the π acceptance of CS and CSe on the substitution of benzene for three carbonyl ligands. The larger π-acceptor/σ-donor ratio of CS and CSe in the benzene complexes is another indicator of the greater charge density on the metal in these compounds compared to the pentacarbonyls. Furthermore, the large variation in this ratio, as reflected in the substantial changes in the force constants of the two series, demonstrates the "charge buffering effect" of CS and CSe, as discussed in the last section. The enhanced π acceptance of CS relative to CO in the benzene complexes can be attributed to the stability of the π^* orbitals of CS which permits greater overlap between these orbitals and the filled metal dπ orbitals, allowing a greater amount of charge to be

(21) M. A. Andrews, *Inorg. Chem.*, **16**, 496 (1977).
(22) B. E. Bursten and R. F. Fenske, *Inorg. Chem.*, **18**, 1760 (1979).
(23) D. A. Brown and R. M. Rawlinson, *J. Chem. Soc. A*, 1534 (1968).
(24) D. G. Carroll and S. P. *McGlynn, Inorg. Chem.*, **7**, 1285 (1968).
(25) D. A. Brown, N. J. Fitzpatrick, and N. J. Mathews, *J. Organomet. Chem.*, **88**, C27 (1975).
(26) N. J. Fitzpatrick, J. M. Savariault, and J. M. R. Labarre, *J. Organomet. Chem.*, **127**, 325 (1977).
(27) M. F. Guest, I. H. Hillier, B. R. Higginson, and D. R. Lloyd, *Mol. Phys.*, **29**, 113 (1975).
(28) D. A. Brown and R. M. Rawlinson, *J. Chem. Soc. A*, 1530 (1969).
(29) S. Pignataro, A. Foffani, and G. Distefano, *Chem. Phys. Lett.*, **20**, 350 (1973).
(30) L. H. Jones, *J. Mol. Spectrosc.*, **36**, 398 (1970).
(31) I. S. Butler, A. Garcia-Rodriguez, K. R. Plowman, and C. F. Shaw III, *Inorg. Chem.*, **15**, 2602 (1976).

Table IX. Comparison of the $[MC(X)]_{CX}$ and $(CX)_{MC(X)}$ Interaction Coordinates for the $BzCr(CO)_2(CX)$ and $Cr(CO)_5(CX)$ (X = O, S, Se) Molecules[a,b]

complex	$[MC(X)]_{CX}$	$(CX)_{MC(X)}$
$Cr(CO)_6$	−0.401	−0.0446
$Cr(CO)_5(CS)$	−0.174	−0.0470
$Cr(CO)_5(CSe)$	−0.131	−0.0501
$BzCr(CO)_3$	−0.354	−0.0470
$BzCr(CO)_2(CS)$	−0.151	−0.0631
$BzCr(CO)_2(CSe)$	−0.110	−0.0663

[a] $Cr(CO)_5(CX)$ data from ref 2. [b] The interaction coordinates are dimensionless for stretch-stretch interactions.

Table X. Diagonal Elements of the Potential Energy Distribution for the Normal Isotopic Species of $(\eta^6\text{-}C_6H_6)Cr(CO)_3$[a-d]

a_1	ν_1 $0.99S_1$	e	ν_9 $1.00S_9$
	ν_2 $0.40\underline{S_2} + 0.23S_3$		ν_{10} $0.68S_{10}$
	ν_3 $0.27S_2 + 0.69\underline{S_3}$		ν_{11} $0.10S_{10} + 0.62\underline{S_{11}} + 0.12S_{12} + 0.15S_{16}$
	ν_4 $0.89S_4$		ν_{12} $0.11S_{11} + 0.60\underline{S_{12}} + 0.13S_{13}$
	ν_5 $0.52S_5 + 0.53S_6$		ν_{13} $0.14S_{12} + 0.70\underline{S_{13}}$
	ν_6 $0.48S_2 + 0.48S_5 + 0.48S_6$		ν_{14} $0.23S_{12} + 0.21S_{13} + 0.10S_{14} + 0.10S_{15} + 0.61\underline{S_{16}}$
a_2	ν_7 $0.90S_7$		ν_{15} $0.81\underline{S_{15}} + 0.18S_{16}$
	ν_8 $0.13S_7 + 0.99\underline{S_8}$		ν_{16} $0.10S_{10} + 0.34\underline{S_{11}} + 1.04S_{14} + 0.18S_{16}$

[a] The symmetry coordinates, S_i, are defined in Table II. [b] The coefficients of S_i, $V_{ij,k}$ give the contribution of S_i to the potential energy of the normal mode, ν_k. [c] Contributions less than 0.10 are omitted. [d] The major contribution to a mixed mode is underlined.

transferred to the CS group. The π-acceptor ability of CSe is expected to arise from the same factors because of the similarity of the two ligands.

The introduction of a CS or CSe group into $BzCr(CO)_3$ causes a large decrease in the metal–ring stretching constant (F_T), which varies from 1.19 mdyn Å^{-1} in the tricarbonyl to 0.897 mdyn Å^{-1} in the selenocarbonyl. This weakening of the metal–ring interaction is probably due to a decrease in the back-bonding to e_2 orbitals (antibonding) of benzene, as these orbitals are not expected to compete favorably with the low-lying π* orbitals of the CS or CSe ligands for the dπ electrons of the metal.[22]

The $[MC(X)]_{CX}$ and $(CX)_{MC(X)}$ interaction coordinates show the same trends as their $Cr(CO)_5(CX)$ counterparts.[2] However, owing to changes in the primary compliants, the values for $[MC(X)]_{CX}$ are somewhat reduced from their corresponding $Cr(CO)_5(CX)$ values, whereas the $(CX)_{MC(X)}$ values are larger (Table IX). The increase in $(CX)_{MC(X)}$ implies a greater reduction in the CX bond length in the $BzCr(CO)_2(CX)$ molecules compared to the $Cr(CO)_5(CX)$ molecules as the adjacent MC(X) bond is stretched. This is consistent with the greater dπ–pπ* overlap in the benzene series, since a decrease in this overlap, which is responsible for the shortening of the CX bond, should be proportional to its magnitude in the first place.

The factors that contribute to the reduction in the $[MC(X)]_{CX}$ values for the benzene series are less apparent. An obvious suggestion is that the various compensatory effects (see ref 2) cancel each other to a greater extent in the $BzCr(CO)_2(CX)$ molecules. However, rationalization of these effects in MO terms will not be possible until the energy levels in both series are known in more detail.

It should be borne in mind, however, that these interaction coordinates are those of a vibrational model of the molecules in which all the interaction constants are constrained to their corresponding values in the hexa- and pentacarbonyls.

Potential Energy Distributions for the $BzCr(CO)_2(CX)$ Molecules. The contributions of the symmetry coordinates ($V_{ii,k}$) to the potential energy of the normal modes are listed

Table XI. Diagonal Elements of the Potential Energy Distribution for the Normal Isotopic Species of the $(\eta^6\text{-}C_6H_6)Cr(CO)_2(CX)$ (X = S, Se) Molecules[a-d]

	ν_k	$(\eta^6\text{-}C_6H_6)Cr(CO)_2(CS)$	$(\eta^6\text{-}C_6H_6)Cr(CO)_2(CSe)$
a′	ν_1	$1.00S_1$	$1.00S_1$
	ν_2	$0.81\underline{S_2} + 0.28S_7$	$0.63\underline{S_2} + 0.47S_7$
	ν_3	$0.58S_3$	$0.62S_3$
	ν_4	$0.43\underline{S_4} + 0.11S_5$	$0.37\underline{S_4} + 0.17S_5$
	ν_5	$0.11S_4 + 0.24\underline{S_5} + 0.12S_6 + 0.12S_7 + 0.12S_{13}$	$0.22S_4 + 0.28\underline{S_5} + 0.11S_6 + 0.13S_{13}$
	ν_6	$0.50\underline{S_6} + 0.28S_7$	$0.73S_6$
	ν_7	$0.12S_4 + 0.27\underline{S_5} + 0.23S_6 + 0.17S_7$	$0.18S_2 + 0.10S_5 + 0.27S_7 + 0.27S_9$
	ν_8	$0.15S_8 + 0.58\underline{S_9}$	$0.33S_8 + 0.31S_9$
	ν_9	$0.70\underline{S_8} + 0.23S_9$	$0.50\underline{S_8} + 0.36S_9$
	ν_{10}	$0.10S_{10} + 0.28S_{12} + 0.54\underline{S_{14}}$	$0.14S_{10} + 0.10S_{11} + 0.22S_{12} + 0.50\underline{S_{14}}$
	ν_{11}	$0.11S_5 + 0.10S_7 + 0.40\underline{S_{10}} + 0.14S_{11} + 0.10S_{12} + 0.21S_{13}$	$0.58\underline{S_{10}} + 0.14S_{11} + 0.11S_{12} + 0.20S_{14}$
	ν_{12}	$0.37S_3 + 0.13S_7 + 0.33S_{10} + 0.56\underline{S_{13}}$	$0.30S_3 + 0.27S_7 + 0.12S_{10} + 0.69\underline{S_{13}}$
	ν_{13}	$0.31S_4 + 0.13S_5 + 0.17S_{10} + 0.44\underline{S_{11}} + 0.11S_{12} + 0.17S_{14}$	$0.30S_4 + 0.17S_{10} + 0.57\underline{S_{11}} + 0.12S_{14}$
	ν_{14}	$0.22S_5 + 0.38S_{11} + 0.52\underline{S_{12}} + 0.24S_{13} + 0.13S_{14}$	$0.31S_5 + 0.24S_{11} + 0.57\underline{S_{12}} + 0.24S_{13} + 0.19S_{14}$
a″	ν_{15}	$1.01S_{15}$	$1.01S_{15}$
	ν_{16}	$0.24S_{16} + 0.33\underline{S_{18}}$	$0.16S_{16} + 0.42\underline{S_{18}}$
	ν_{17}	$0.55\underline{S_{17}} + 0.10S_{16} + 0.10S_{19}$	$0.64\underline{S_{16}} + 0.20S_{18}$
	ν_{18}	$0.50\underline{S_{16}} + 0.36S_{18}$	$0.48\underline{S_{17}} + 0.16S_{19}$
	ν_{19}	$0.18S_{17} + 0.68\underline{S_{19}}$	$0.27S_{17} + 0.60\underline{S_{19}}$
	ν_{20}	$0.85S_{20}$	$0.86S_{20}$
	ν_{21}	$0.19S_{17} + 0.18S_{19} + 0.10S_{20} + 0.10S_{21} + 0.32\underline{S_{22}} + 0.10S_{23} + 0.23S_{24}$	$0.19S_{17} + 0.17S_{19} + 0.10S_{20} + 0.10S_{21} + 0.31\underline{S_{22}} + 0.26S_{24}$
	ν_{22}	$0.10S_{16} + 0.13S_{18} + 0.13S_{21} + 0.37S_{22} + 0.58\underline{S_{24}}$	$0.11S_{16} + 0.12S_{18} + 0.15S_{21} + 0.47S_{22} + 0.50\underline{S_{24}}$
	ν_{23}	$0.25S_{22} + 0.95\underline{S_{23}}$	$0.16S_{21} + 0.16S_{22} + 0.95\underline{S_{22}}$
	ν_{24}	$0.20S_{18} + 0.75\underline{S_{21}} + 0.12S_{22} + 0.20S_{24}$	$0.29S_{18} + 0.65\underline{S_{21}} + 0.16S_{22} + 0.25S_{24}$

[a] S_i is defined in Table III. [b] See footnotes b–d of Table X.

Table XII. CO and CX Force Constants and (CO,CO) Interaction Constants for the (η^6-C_6H_6)$Cr(CO)_2$(CX) (X = O, S, Se) Molecules for Some Approximate Force Fields[a,b]

F[c]	anhar EF[d]	har EF	har GQ[e]
	$BzCr(CO)_3$		
F_D	15.01	15.36	15.41
F_{DD}	0.378	0.374	0.3021
	$BzCr(CO)_2(CS)$		
F_D	15.30	15.69	15.77
F_{DD}	0.356	0.372	0.314
F_{D_X}	7.647	7.849	6.528
	$BzCr(CO)_2(CSe)$		
F_D	15.41	15.81	15.89
F_{DD}	0.344	0.350	0.305
F_{D_X}	6.905	7.062	4.757

[a] Units in mdyn $Å^{-1}$. [b] ν(CO) and ν(CX) frequencies from CS_2 solution data, Tables IV-VII. [c] D = CO, D_X = CX. [d] EF = energy factored. [e] GQ = general quadratic.

in Tables XI and XII. The PED for the tricarbonyl is similar to that observed for $Cr(CO)_6$.[20] This is partly due to the starting values for the C_{ij} and the constraints imposed on them in the calculation. As in the hexacarbonyl,[20] the ν(MC) and δ(MCO) modes are strongly coupled in the bands appearing at ca. 650–400 cm^{-1}. The angle bending modes are also highly mixed and contain some δ(MCO), ν(MC), and ν(ML) character as well. Little mixing of the MC and ML stretches is indicated but, given that the calculated degree of mixing depends to a large extent on the value assumed for the (MC,ML) interaction constant which was somewhat arbitrarily set equal to the (MC,MC) interaction of $Cr(CO)_6$, some doubt must remain about the mixing of these modes.

The PED's of $BzCr(CO)_2(CX)$ compared to those of $Cr(CO)_5(CX)$[2] reveal a large increase in mixing of the CX and MC(X) modes in the arene complexes. Since this means that the CS and CSe stretching modes contain an even greater amount of MC(X) stretching than the corresponding modes of $Cr(CO)_5(CX)$, energy factoring is expected to be an even worse approximation here. The CO and CS or CSe stretches do not mix, which was also observed to be the case for $Cr(CO)_5(CX)$. On the other hand, $\delta(MCO)_\parallel$ and $\delta(MCX)_\parallel$ are almost completely mixed in the A′ block and the same holds true for $\delta(MCO)_\perp$ and $\delta(MCX)_\perp$ in the A″ block. As discussed above, this is reflected in the isotopic behavior of these linear bending modes. It should also be noted that the MC and ML stretches again show little mixing in either the thio- or selenocarbonyl compounds. This is not surprising since the (MC,ML) interaction force constant was not adjusted in the C_s calculations.

Energy-Factored Force Fields (EFFF). The harmonic and anharmonic ν(CO) and ν(CX) frequencies[18] were used to determine EFFF for the $BzCr(CO)_2(CX)$ molecules, and the results are given in Table XII. The effects of CO-energy factoring and the neglect of anharmonicity on the primary CO and the (CO,CO) interaction constants are the same as those found for $Cr(CO)_5(CX)$.[2] The (CO,CO) interaction in question is equivalent to the cis (CO,CO) constant of $Cr(CO)_5(CX)$.

It is clear from a comparison of the CX stretching force constants for the various approximations that an even greater difference exists between the general quadratic and energy-factored values for $BzCr(CO)_2(CX)$ than for $Cr(CO)_5(CX)$. This is especially true for the selenocarbonyls where ΔF (energy-factored—general quadratic) is 1.65 and 2.305 mdyn $Å^{-1}$ for $Cr(CO)_5(CSe)$ and $BzCr(CO)_2(CSe)$, respectively. Such variation certainly shows that energy-factored force constants for the ν(CX) modes of coordinated CS and CSe do not form a valid basis for comparison between different molecules as is possible in the case of CO. Furthermore, attempts to correlate other parameters (e.g., NMR chemical shifts) with either the observed CX stretching vibrations of the CX energy-factored force constants are rather pointless, although some fortuitous trends may well be observed.

Acknowledgment. This work was generously supported by the Natural Sciences and Engineering Research Council of Canada and le Gouvernement du Québec (Ministère de l'Education).

Registry No. $BzCr(CO)_3$, 12082-08-5; (Bz-d_6)$Cr(CO)_3$, 38095-88-4; $BzCr(^{13}CO)_3$, 76374-48-6; $BzCr(CO)_2(CS)$, 63356-86-5; (Bz-d_6)$Cr(CO)_2(CS)$, 79467-16-6; $BzCr(^{13}CO)_2(CS)$, 76380-94-4; $BzCr(CO)_2(^{13}CS)$, 79483-61-7; $BzCr(CO)_2(CSe)$, 63356-85-4; (Bz-d_6)$Cr(CO)_2(CSe)$, 79483-62-8; $BzCr(^{13}CO)_2(CSe)$, 76380-93-3.

Supplementary Material Available: the primary symmetry compliants for (η^6-C_6H_6)$Cr(CO)_2$(CX) [Table 13(s), X = O; Table 14(s), X = S and Se], the initial and final symmetry compliants, for the same molecules [Table 15(s), X = O; Table 16(s), X = S and Se], the wavenumber errors for the calculated fundamental modes of the (η^6-C_6H_6)$Cr(^{12}CO)_2(^{12}CX)$ (X = O, S, Se) molecules and their various ^2H- and ^{13}C-labeled derivatives [Table 17(s)], and the valence compliance constants for the (η^6-C_6H_6)$Cr(CO)_2$(CX) (X = O, S, Se) molecules and the $Cr(CO)_6$ equivalents [Table 18(s)] (12 pages). Ordering information is given on any current masthead page.